

Stereoselective Rhodium-Catalyzed [3 + 2 + 1] Carbocyclization of Alkenylidenecyclopropanes with Carbon Monoxide: Theoretical Evidence for a Trimethylenemethane Metallacycle Intermediate

Shivnath Mazumder,[†] Deju Shang,[§] Daniela E. Negru,[§] Mu-Hyun Baik,^{*,†,‡} and P. Andrew Evans^{*,§}

[†]Department of Chemistry, Indiana University, 800 East Kirkwood Avenue, Bloomington, Indiana 47405, United States

[‡]Department of Chemistry, Korea University, 208 Seochang, Chochiwon, Chung-nam 339-700, South Korea

[§]Department of Chemistry, The University of Liverpool, Liverpool L69 7ZD, United Kingdom

S Supporting Information

ABSTRACT: The theoretically inspired development of a Rh-catalyzed [3 + 2 + 1] carbocyclization of carbon- and heteroatom-tethered alkenylidenecyclopropanes (ACPs) with CO for the stereoselective construction of cis-fused bicyclohexenones is described. This study demonstrates that the ring opening of alkyldenecyclopropane proceeds through a Rh(III)–trimethylenemethane complex, which undergoes rate-determining carbometalation through a transition state that accurately predicts the stereochemical outcome for this process. The experimental studies demonstrate the validity of this approach and include the first highly enantioselective reaction involving an ACP to highlight further the synthetic utility of this transformation.

The design and implementation of new metal-catalyzed higher-order carbocyclization reactions, which combine three or more π -fragments, provides a powerful strategy for target-directed synthesis.^{1,2} Notwithstanding the inherent utility of this approach, the ability to join the π -components in a chemo-, regio-, and stereoselective manner remains challenging due to the limited understanding of the factors that control the selectivity. We³ and others⁴ have demonstrated the importance of theoretical studies that predict reaction barriers and thereby provide the basis for experimental studies. For example, we recently demonstrated for the Pauson–Khand (PK) reaction that the barrier for the rate-determining step could be lowered by modifying the stereochemicals of the 1,6-enyne^{3d} and that the degree of stereocontrol could be improved using a five-coordinate Rh complex.^{3b} In a related program, we developed a Rh-catalyzed [3 + 2 + 2] carbocyclization of alkenylidenecyclopropanes (ACPs) with alkynes for the construction of cis-fused bicycloheptadienes.⁵ We envisioned that the combination of these programs would provide an opportunity to develop a new type of carbocyclization reaction. Herein we describe the combined theoretical and experimental development of a Rh-catalyzed [3 + 2 + 1] carbocyclization of ACPs **1** with CO to provide cis-fused bicyclohexenones **3** in a highly efficient and stereoselective manner (Scheme 1).⁶

Devising a reliable computer model without knowing the exact composition of the catalytically active species requires the evaluation of many possible metal complexes to identify the active catalyst. In this context, we examined the effect of PPh₃ with CO

Scheme 1. Rh-Catalyzed [3 + 2 + 1] Carbocyclization Reaction with Various Carbon and Heteroatom Tethers

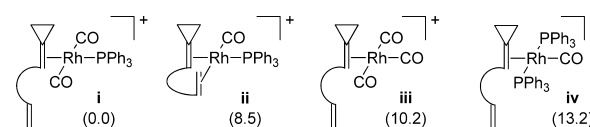
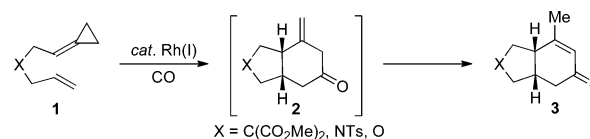


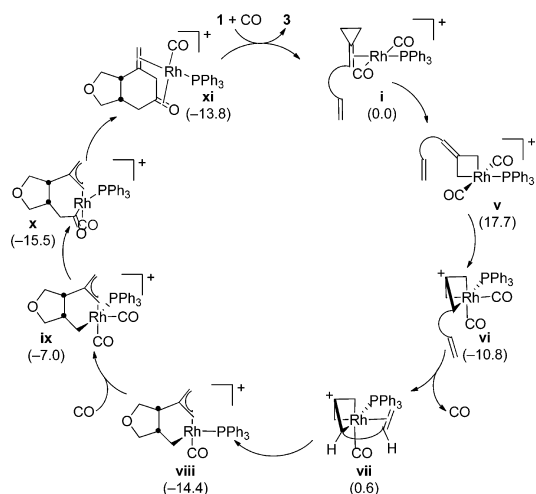
Figure 1. Square-planar Rh(I) complexes examined. Solution-phase Gibbs free energies $\Delta G(\text{Sol})$ (in kcal/mol) are given in parentheses.¹⁰

ligands bound to Rh and the ACP fragment to determine the impact of the various combinations. Figure 1 summarizes the relative energies of four plausible complexes, among which complex **i** with the PPh₃ ligand trans to the olefin of the ACP is significantly more stable than the related complexes **ii–iv** and provides the most mechanistically relevant complex for this synthetic transformation (vide infra).^{7,8} These findings also provide important insight into the dichotomy in reactivity between neutral and cationic complexes in the Rh variant of the PK reaction (see the Supporting Information).^{2,9}

Scheme 2 outlines the proposed catalytic cycle. The formation of complex **i** promotes oxidative addition to afford square-pyramidal rhodacyclobutane **v**, which is 17.7 kcal/mol higher in energy than the reactant complex and has an associated transition state **i-TS** at 23.0 kcal/mol (Figure 2). These energies are surprising at first sight, as previous studies established that the metallacycle-forming oxidative addition for these classes of molecules is typically downhill because of the strong Rh–C bonds formed during the reaction.^{3,11} The alternative pathway, which requires an oxidative addition involving the proximal C–C bond of the three-membered ring of the ACP, was found to be too high in energy. Ring opening of the ACP without the involvement of a rhodacyclobutane intermediate is also energetically irrelevant.⁷ Exploring the potential energy surface more carefully, we found that **v** unexpectedly rearranges to afford **vi**,

Received: June 12, 2012

Published: August 28, 2012

Scheme 2. Proposed Catalytic Cycle^a

^aNumbers in parentheses are $\Delta G(\text{Sol})$ values in kcal/mol.

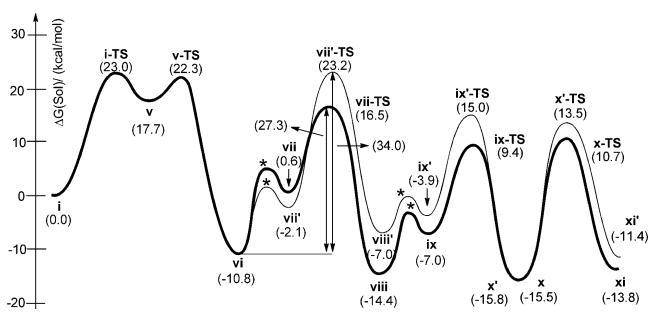


Figure 2. Diastereospecific reaction energy profiles for the Rh-catalyzed [3 + 2 + 1] carbocyclization. The bold and lightface profiles are for the cis- and trans-fused bicyclic systems, respectively. Transition states indicated by * were not explicitly located and are shown for illustration only.

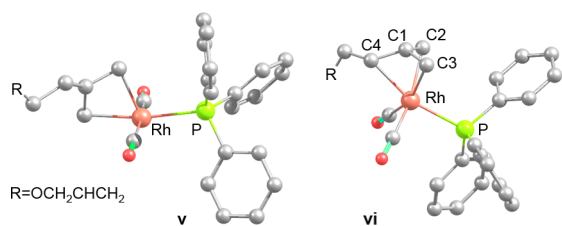


Figure 3. Optimized geometries of intermediates **v** and **vi**. H atoms have been omitted for clarity.

a six-coordinate 18-electron Rh(III) trimethylenemethane (TMM) complex. Although this intermediate was unanticipated, this type of complex is known.¹² Figure 3 illustrates the optimized geometries of highly strained rhodacyclobutane intermediate **v** and Rh(III)–TMM complex **vi**. The TMM moiety binds facially to Rh to provide a three-legged piano stool type of coordination. The binding is essentially symmetric with respect to C1–C2, C1–C3, and C1–C4, since these bond distances are essentially equal (1.436, 1.438, and 1.433 Å, respectively). We propose that **vi** is the resting state of the catalytic cycle. To force the reaction forward and promote C–C coupling, one CO ligand must dissociate to expose a binding site for the pendant vinyl moiety, affording **vii**, which is ~10 kcal/mol higher in energy than **vi**. The metal undergoes stereoselective carbometalation on the vinyl group to furnish cis-fused bicycle **viii**, traversing the transition

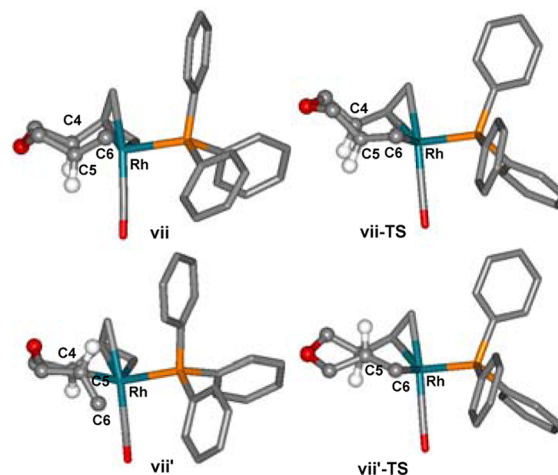


Figure 4. Structures of the diastereomeric intermediates **vii** and **vii'** and transition states **vii-TS** and **vii'-TS**. The H atoms at C4 and C5 are depicted in white, and the others have been omitted for clarity.

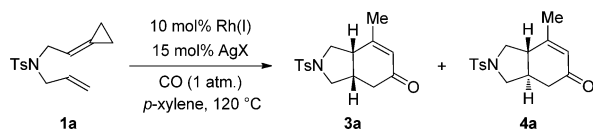
state **vii-TS** at 16.5 kcal/mol. Figure 4 highlights the structural differences in the two transition states, in which the insertion of the vinyl group (C5–C6) results in C4–C5 bond formation. The relative orientation of the two hydrogens at the ring junction (C4 and C5) is syn in **vii-TS** and anti in **vii'-TS**, with the syn diastereoisomer preferred by ~7 kcal/mol. Structurally, the C4...C5 distance of 3.34 Å in **vii'** is notably longer than that of 3.22 Å in **vii** and becomes shorter in **vii'-TS** (2.05 Å) than in **vii-TS** (2.13 Å). As illustrated in Figure 4, the tether in **vii** adopts a classical chair-type envelope structure that is maintained in the transition state **vii-TS**, while the conformation of the tether for the other diastereoisomer changes significantly from envelope in **vii'** to twisted boat in **vii'-TS**. This change in the conformation accounts for the higher activation energy required for the anti orientation of the two hydrogens. To complete the catalytic cycle, migratory insertion of a carbonyl in **viii** requires addition of another ligand, which we propose to be a CO ligand, to form the six-coordinate Rh(III) species **ix**. Migratory insertion of a carbonyl into the Rh–C bond gives intermediate **x**, traversing the transition state **ix-TS** at 9.4 kcal/mol. Reductive elimination and concomitant C–C coupling yields the product complex **xi**. This step is associated with a barrier of 26 kcal/mol. Finally, a 1,3-hydride shift leads to an isomerization of the exocyclic olefin to afford the desired endocyclic olefin. Our calculations invoke a Rh(III)–hydride intermediate and a very reasonable barrier of ~15 kcal/mol (see the Supporting Information for details).¹³ We also probed the fate of the mechanism proposed in Scheme 2 in the presence of CO ligands without any phosphine present on the Rh center. Replacement of the electron-donating PPh₃ ligand with an electron-withdrawing CO ligand makes the Rh center electron-deficient, and as a result, the energy of transition state for the insertion of the vinyl moiety becomes higher than that of **vii-TS**.⁷

Hence, the computational studies suggest that insertion of the vinyl group (**vi** → **viii**) is most likely the rate-determining step in the catalytic cycle. This finding is distinctively different from those for related reactions, such as the Rh(I)-catalyzed [2 + 2 + 1] carbocyclization^{2,3b,d} and related metal-catalyzed [2 + 2 + 2] reactions,^{11,14} where the initial oxidative addition step is rate-determining.⁷ The shift in mechanism is a direct result of the energy released in ring opening of the ACP (**i** → **vi**), which makes the oxidative addition significantly more favorable. The

ACP group also decouples C–C bond formation from the oxidative addition step, thereby delegating the installation of the stereocenter(s) to a later phase of the catalytic cycle. As we demonstrated previously,^{3b,d} coupling the stereochemistry-determining C–C bond formation to the oxidative addition necessarily gives control of the stereochemistry to the electronics of the metal center, whereas when these two events are decoupled, as described above, the stereochemistry is primarily substrate-controlled. This subtle yet decisive distinction is important and provides the mechanistic hypothesis for the following experimental studies to validate the theoretical work.

Encouraged by the theoretical prediction that the [3 + 2 + 1] carbocyclization is associated with reasonable barriers and, more importantly, that it should favor the *cis*-fused bicyclohexenones **3**, we initiated experimental studies, focusing first on validating the computed catalyst selection. Treatment of ACP **1a** with the catalyst derived from [Rh(CO)₂Cl]₂ and triphenylphosphine in the presence of CO furnished *cis*-fused bicyclohexenone **3a** in 68% yield with ≥19:1 diastereoselectivity, which was confirmed by X-ray crystallographic analysis (Table 1, entry 1). Interestingly, adding more phosphine or a bidentate ligand gave similar results, albeit with

Table 1. Optimization of the Rh-Catalyzed Carbocyclization^a



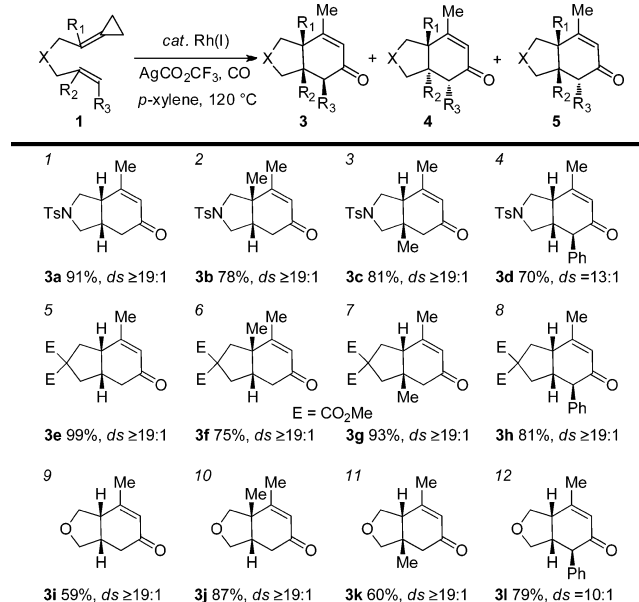
entry	rhodium complex	ligand (M:L)	AgX	yield (%) ^b	<i>ds</i> 3a/4a ^c
1	[Rh(CO) ₂ Cl] ₂	PPh ₃ (1:1)	-	68	≥19:1
2	"	PPh ₃ (1:2)	-	41	≥19:1
3	"	dppp (1:1)	-	53	≥19:1
4	Rh(CO)(PPh ₃) ₂ Cl	-	-	55	≥19:1
5	"	-	AgPF ₆	86	≥19:1
6	Rh(PPh ₃) ₃ Cl	-	-	53	≥19:1
7	"	-	AgPF ₆	86	≥19:1
8	"	-	AgCO ₂ CF ₃	91	≥19:1

^aAll reactions were carried out on a 0.1 mmol scale at 0.05 M. ^bIsolated yields. ^cDetermined by ¹H NMR analysis of the crude products.

slightly lower yields (entries 2 and 3), supporting the theoretical results discussed above. The proposed catalytic cycle employs a cationic complex, which is likely to be significantly more reactive. In this context, we elected to use a mixed-ligand species to probe the effect of neutral and cationic species. The cationic species was superior (entry 5 vs 4), which is consistent with the computational studies and related synthetic studies on the Rh-catalyzed PK reaction.^{2,7,9} In line with this reasoning, we elected to complete the study using Wilkinson's catalyst. Gratifyingly, the cationic variant performed in an analogous manner (entry 7 vs 6), further supporting the mechanistic hypothesis. Finally, the optimal reaction conditions employed a rather unusual silver salt, silver trifluoroacetate, which provided **3a** in 91% overall yield (entry 8).

Table 2 outlines the application of the optimized reaction conditions (Table 1, entry 8) to carbon- and heteroatom-tethered ACPs **1** to illustrate the synthetic scope of this reaction. Interestingly, the bridgehead diastereoselectivity is independent of the nature of the ACP tether, alkene geometry, and substitution, albeit the oxygen tethers are generally less efficient (entries 1 and 5 vs 9), again supporting the theoretically derived notion that the tether portion of the substrate is not directly engaged with the metal center in the rate-determining step. This process

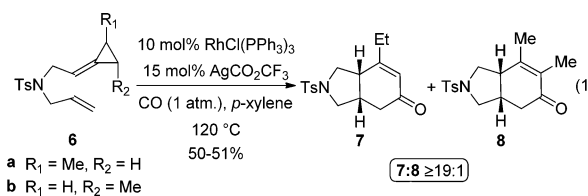
Table 2. Scope of the Rh-Catalyzed Carbocyclization^a



^aAll reactions were carried out on a 0.1 mmol scale using RhCl(PPh₃)₃ (10 mol %) and AgCO₂CF₃ (15 mol %) under CO (1 atm) in *p*-xylene (0.05 M) at 120 °C for ~12 h. Isolated yields are shown. *ds* values were determined by ¹H NMR analysis of the crude products.

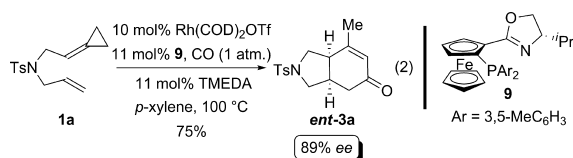
provides unparalleled versatility with regard to the ability to install a bridgehead quaternary carbon stereogenic center (entries 2, 6, and 10 vs 3, 7, and 11), which is likely to have significant utility for synthetic applications. Furthermore, the cycloisomerization of trisubstituted alkenes provides an additional stereogenic center (entries 4, 8, and 12), albeit with slightly lower diastereocontrol from the epimerization of **3** to provide **5**. In contrast, the *cis*-alkene is unreactive, confirming that the process is stereospecific. Overall, the experimental studies confirm the theoretical hypothesis and provide a highly diastereoselective approach to functionalized *cis*-fused bicyclohexenones, which represent important synthetic intermediates.

On the basis of the proposed mechanism, we envisioned that ACPs **6a** and **6b** would provide additional evidence for the π -allyl intermediates **viii**–**x**. For instance, selective formation of **7** or **8** would be consistent with a stereospecific reductive elimination of **x**, whereas the exclusive formation of **7** would demonstrate that the π -allylrhodium species is fluxional and can preferentially undergo reductive elimination from the less sterically hindered terminus.⁷ Treatment of **6a** and **6b** under standard reaction conditions furnished the *cis*-fused bicyclohexenone **7** (eq 1), which supports the intermediacy of a fluxional π -allyl intermediate. Hence, the ability to modify the β -position of the bicyclohexenone selectively in this manner provides important scope for this transformation.



Finally, we envisioned that the development of an enantioselective variant would further highlight the synthetic utility of this

process. Interestingly, there are relatively few examples of enantioselective reactions involving ACPs,¹⁵ which is consistent with the theoretical preference for a monodentate phosphine ligand. Nevertheless, analysis of our computed mechanism coupled with the insight gained from the experimental results suggested that the enantiodetermining step, $\mathbf{v} \rightarrow \mathbf{vi}$, may be able to tolerate a bidentate ligand. Gratifyingly, treatment of ACP **1a** with the catalyst derived from Rh(COD)₂OTf and the chiral P,N-ligand^{16,17} **9** in the presence of CO and tetramethylethylenediamine (TMEDA)¹⁸ furnished cis-fused bicyclohexenone **ent-3a** in 75% yield with 89% enantiomeric excess (eq 2). This represents the first highly enantioselective reaction involving an ACP and provides an important proof-of-principle for related transformations that contain this motif.



In conclusion, we have developed a novel Rh-catalyzed [3 + 2 + 1] carbocyclization reaction using theory to predict the catalytic requirements and the critical steps in the catalytic cycle that impact enantio- and diastereoselectivity. The mechanistic understanding garnered from this study provided a robust hypothesis for the subsequent experimental studies. For example, the theoretical analysis predicted the optimal metal complex, which provided important insight into the precatalyst requirements for reactions involving CO. Moreover, the theoretical studies indicated that the stereodetermining steps occur at different points in the catalytic cycle, permitting enantio- and diastereoselective variants to be developed. Additional studies provided evidence for the intermediacy of a fluxional π -allylrhodium complex, permitting substitution at the β -position of the bicyclohexenone.

■ ASSOCIATED CONTENT

Supporting Information

Computational details and results, experimental procedures, characterization data, and CIF files for **3a**, **3h**, and **ent-3a**. This material is available free of charge via the Internet at <http://pubs.acs.org>.

■ AUTHOR INFORMATION

Corresponding Author

mbaik@indiana.edu; Andrew.Evans@liverpool.ac.uk

Notes

The authors declare no competing financial interest.

■ ACKNOWLEDGMENTS

We thank the EPSRC (EP/G010250) and NSF (CHE-0645381 and CHE-1001589) for financial support, the Royal Society for a Wolfson Research Merit Award (P.A.E.), the Research Corporation for a Cottrell Scholarship and Scialog Award (M.-H.B.), the WCU Program of the National Research Foundation of Korea (M.-H.B.), and the EPSRC National Mass Spectrometry Service Centre (Swansea, U.K.) for HR-MS analyses.

■ REFERENCES

(1) For recent reviews of higher-order carbocyclization reactions, see: (a) Inglesby, P. A.; Evans, P. A. *Chem. Soc. Rev.* **2010**, *39*, 2791. (b) Aubert, C.; Malacria, M.; Ollivier, C. *Sci. Synth.* **2011**, *3*, 145 and references cited therein.

(2) For recent reviews of PK-type reactions, see: (a) Perez-Castells, J. *Top. Organomet. Chem.* **2006**, *19*, 207. (b) Lee, H.-W.; Kwong, F.-Y. *Eur. J. Org. Chem.* **2010**, 789. (c) Shibata, T. *Sci. Synth.* **2011**, *3*, 125 and references cited therein.

(3) (a) Baik, M.-H.; Baum, E. W.; Burland, M. C.; Evans, P. A. *J. Am. Chem. Soc.* **2005**, *127*, 1602. (b) Wang, H.; Sawyer, J. R.; Evans, P. A.; Baik, M.-H. *Angew. Chem., Int. Ed.* **2008**, *47*, 342. (c) Pitcock, W. H., Jr.; Lord, R. L.; Baik, M.-H. *J. Am. Chem. Soc.* **2008**, *130*, 5821. (d) Baik, M.-H.; Mazumder, S.; Ricci, P.; Sawyer, J. R.; Song, Y.-G.; Wang, H.; Evans, P. A. *J. Am. Chem. Soc.* **2011**, *133*, 7621.

(4) (a) Yu, Z.-X.; Wender, P. A.; Houk, K. N. *J. Am. Chem. Soc.* **2004**, *126*, 9154. (b) Wang, Y.; Wang, J.; Su, J.; Huang, F.; Jiao, L.; Liang, Y.; Yang, D.; Zhang, S.; Wender, P. A.; Yu, Z.-X. *J. Am. Chem. Soc.* **2007**, *129*, 10060. (c) Houk, K. N.; Cheong, P. H.-Y. *Nature* **2008**, *455*, 309. (d) Yu, Z.-X.; Cheong, P. H.-Y.; Liu, P.; Legault, C. Y.; Wender, P. A.; Houk, K. N. *J. Am. Chem. Soc.* **2008**, *130*, 2378. (e) Huang, F.; Yao, Z.-K.; Wang, Y.; Wang, Y.; Zhang, J.; Yu, Z.-X. *Chem.—Asian J.* **2010**, *5*, 1555. (f) Liu, P.; Sirois, L. E.; Cheong, P. H.-Y.; Yu, Z.-X.; Hartung, I. V.; Rieck, H.; Wender, P. A.; Houk, K. N. *J. Am. Chem. Soc.* **2010**, *132*, 10127. (g) Jiao, L.; Lin, M.; Yu, Z.-X. *J. Am. Chem. Soc.* **2011**, *133*, 447. (h) Lin, M.; Li, F.; Jiao, L.; Yu, Z.-X. *J. Am. Chem. Soc.* **2011**, *133*, 1690.

(5) Evans, P. A.; Inglesby, P. A. *J. Am. Chem. Soc.* **2008**, *130*, 12838.

(6) For related metal-catalyzed [3 + 2 + 1] carbocyclization reactions, see: (a) Koga, Y.; Narasaka, K. *Chem. Lett.* **1999**, 705. (b) Jiao, L.; Lin, M.; Zhuo, L.-G.; Yu, Z.-X. *Org. Lett.* **2010**, *12*, 2528. (c) Li, C.; Zhang, H.; Feng, J.; Zhang, Y.; Wang, J. *Org. Lett.* **2010**, *12*, 3082.

(7) See the Supporting Information (SI) for more details and additional comments on other mechanistic pathways probed.

(8) For examples of Pd/Ni-catalyzed carbocyclizations with ACPs, see: (a) Suzuki, T.; Fujimoto, H. *Inorg. Chem.* **2000**, *39*, 1113. (b) Gulías, M.; García, R.; Delgado, A.; Castedo, L.; Mascareñas, J. L. *J. Am. Chem. Soc.* **2006**, *128*, 384. (c) Saya, L.; Bhargava, G.; Navarro, M. A.; Gulías, M.; López, F.; Fernández, I.; Castedo, L.; Mascareñas, J. L. *Angew. Chem., Int. Ed.* **2010**, *49*, 9886. (d) Gulías, M.; López, F.; Mascareñas, J. L. *Pure Appl. Chem.* **2011**, *83*, 495.

(9) (a) Jeong, N.; Lee, S.; Sung, B. K. *Organometallics* **1998**, *17*, 3642. (b) Jeong, N.; Sung, B. K.; Choi, Y. K. *J. Am. Chem. Soc.* **2000**, *122*, 6771.

(10) See the SI for computational details.

(11) (a) Montero-Campillo, M. M.; Rodríguez-Otero, J.; Cabaleiro-Lago, E. *J. Phys. Chem. A* **2008**, *112*, 2423. (b) Dachs, A.; Torrent, A.; Roglans, A.; Parella, T.; Osuna, S.; Solà, M. *Chem.—Eur. J.* **2009**, *15*, 5289. (c) Dachs, A.; Osuna, S.; Roglans, A.; Solà, M. *Organometallics* **2010**, *29*, 562. (d) Dachs, A.; Roglans, A.; Solà, M. *Organometallics* **2011**, *30*, 3151.

(12) For examples of metal-TMM complexes, see: (a) Noyori, R.; Yamakawa, M.; Takaya, H. *Tetrahedron Lett.* **1978**, *19*, 4823. (b) Jones, M. D.; Kemmitt, R. D. W.; Platt, A. W. G. *J. Chem. Soc., Dalton Trans.* **1986**, 1411. (c) Herberich, G. E.; Spaniol, T. P. *J. Chem. Soc., Dalton Trans.* **1993**, 2471. (d) McNeill, K.; Andersen, R. A.; Bergman, R. G. *J. Am. Chem. Soc.* **1997**, *119*, 11244.

(13) See the SI for the mechanism of the isomerization of **2** to **3**.

(14) (a) Yamamoto, Y.; Arakawa, T.; Ogawa, R.; Itoh, K. *J. Am. Chem. Soc.* **2003**, *125*, 12143. (b) Orian, L.; van Stralen, J. N. P.; Bickelhaupt, F. M. *Organometallics* **2007**, *26*, 3816.

(15) Gulías, M.; Durán, J.; López, F.; Castedo, L.; Mascareñas, J. L. *J. Am. Chem. Soc.* **2007**, *129*, 11026.

(16) For the first preparation of this class of ligands, see: (a) Richards, C. J.; Damalidis, T.; Hibbs, D. E.; Hursthouse, M. B. *Synlett* **1995**, 74. (b) Sannakia, T.; Latham, H. A.; Schaad, D. R. *J. Org. Chem.* **1995**, *60*, 10. (c) Nishibayashi, Y.; Uemura, S. *Synlett* **1995**, 79.

(17) Although the enantioselectivity was excellent for this particular example, other substrates provided slightly lower enantioselectivities (e.g., 80% ee for **3e** and **3f**).

(18) The presence of TMEDA is important for catalyst recovery, since we observed significantly reduced turnover frequency in its absence.

■ NOTE ADDED AFTER ASAP PUBLICATION

Revised SI files were posted and refs 8 and 12 were revised on December 13, 2012.